JACS
JOURNAL OF THE AMERICAN CHEMICAL SOCIETY

ARTICLE

pubs.acs.org/JACS

Superhydrophobic Fiber Mats by Electrodeposition of Fluorinated Poly(3,4-ethyleneoxythiathiophene)

Thierry Darmanin and Frédéric Guittard*

Université de Nice — Sophia Antipolis, Equipe Chimie Organique aux Interfaces, Parc Valrose, 06108 Nice Cedex 2, France

Supporting Information

ABSTRACT: The control of surface morphology and wettability is crucial in the development of superhydrophobic surfaces, which implies new strategy and molecular design. In this Article, we report the synthesis, characterization, and electrochemical properties of original 3,4-ethyleneoxythiathiophenes (EOTT) as platform molecules and its derivatives bearing a semifluorinated chain of various length (*F*-octyl, *F*-hexyl, *F*-butyl, and *F*-ethyl). We report the influence of the fluorinated chain length as well as the presence of sulfur atoms in the monomer on the surface construction and nonwetting properties of the corresponding electrodeposited polymer films. Surprisingly, these films exhibit the possibility to obtain extremely long polymer fibers with a possible control of their length by a careful choice in the monomer structure. We show that the presence of sulfur atoms in the monomer structure seems to be necessary to modulate the formation of extremely long polymer fibers by aggregation of smaller polymer fibrils. In this Article, the formation of superhydrophobic material (contact angle above 150°) for four, six, and eight fluoromethylene units but also highly hydrophobic surfaces (contact angle above 125°) from extremely short chains (two fluoromethylene units) is also demonstrated.

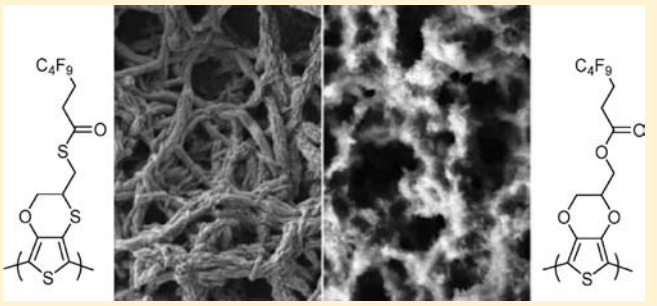

INTRODUCTION

The fabrication of materials from a biomimetic approach is a promising route to reach unequaled properties.[1−4] Hence, combining surface structuration at a micro-/nanoscale with low surface energy materials, it has been possible to produce superhydrophobic surfaces of various potential applications.[5−7] These applications include the domains of self-cleaning transparent windows, water-proof clothes, military uniforms, and anticorrosion surfaces.[8−13] The process of surface structuration can be divided into two global approaches: the top-down (lithography, templating, chemical, plasma, and laser etching) and the bottom-up (sol−gel coatings, electrospinning, electrospray, chemical vapor deposition, layer-by-layer assemblies, electrodeposition).[14−21]

In the literature, conductive polymers were used to reach surfaces with structures of micro-/nano-dimension displaying superhydrophobic properties. Different strategies were elaborated to control the nonwetting properties. For example, dandelion-like microspheres and rambutan-like hollow spheres of polyaniline were obtained by self-assembly.[22−24] Another strategy includes the use of template such as anodic aluminum oxide to form nanowires or nanofibers after template removal.[25−27] Finally, superhydrophobic surfaces were obtained by electrodeposition. The electrodeposition is a cost-effective and reproducible process to form not only metals and metal oxides but also conductive polymers of controllable morphology. In the case of conductive polymers, the hydrophobic part could be included with a post-treatment,[28] with the salt used in the process (conductive polymers are often produce as charged polymers)[29] or in the monomer chemical structure before polymerization.[30−36] Using this last strategy, it has been demonstrated the influence of both surface wettability and morphology with the monomer chemical structure and the electrochemical parameters. Indeed, the control of surface wettability and morphology is crucial for many applications. Hence, surfaces displaying exceptional water-repellency properties (hysteresis and sliding angles below 3°) were obtained from fluorinated EDOT derivatives (Scheme 1a) and with various surface morphologies.[33]

Previously, Roncali et al. showed the possibility to synthesize thieno[3,4-*b*]-1,4-oxathiane or 3,4-ethyleneoxythiathiophene, an unsymmetrical sulfur analogue of EDOT, by reaction of 3,4-dimethoxythiophene and 2-mercaptoethanol in the presence of *p*-toluenesulfonic acid.[37] Here, by replacing 2-mercaptoethanol by 2,3-dimercapto-1-propanol, an original thieno[3,4-*b*]-1,4-oxathiane derivative containing a thiol substituent (Scheme 2) was synthesized and coupled with semifluorinated acids (Scheme 1b: EOTT-F_n with n = 2, 4, 6, and 8). The fluorinated monomers were electrodeposited, and the surface properties were evaluated to determine the influence of the sulfur atoms as well as the fluorinated chain length on surface wettability and morphology. The monomer EOTT-H was also synthesized to determine the influence of the presence of the fluorinated chain.

Received: June 8, 2011
Published: August 26, 2011

EXPERIMENTAL SECTION

Monomer Synthesis. The synthetic way to the fluorinated monomers EOTT-F_n and EOTT-H is represented in Scheme 2. 4,4,5,5,5-Pentafluoropentanoic acid was purchased from Fisher Acros Organics. The other chemicals were obtained from Sigma-Aldrich. Some characterization data are given in the Supporting Information.

Synthesis of (2,3-Dihydrothieno[3,4-b][1,4]oxathiin-3-yl)methanethiol. 3,4-Dimethoxythiophene (0.8 g, 5.5 mmol), 2,3-dimercapto-1-propanol (0.55 mL, 5.5 mmol), and *p*-toluenesulfonic acid (30 mg) were added in 20 mL of toluene. Next, 5.5 mmol of 2,3-dimercapto-1-propanol was added twice after stirring at 80 °C during 1 and 2 days. After, the solvent was removed and the crude was purified by column chromatography (silica gel; eluent: cyclohexane/ethyl acetate 9:1) to yield the product as a colorless liquid.

Yield 30%; r.t. 12.6 min; colorless liquid. δ_H (200 MHz, $CDCl_3$, ppm): 6.73 (d, $^4J_{HH}$ = 3.5 Hz, 1H), 6.50 (d, $^4J_{HH}$ = 3.5 Hz, 1H), 4.57 (dd, $^2J_{HH}$ = 11.7 Hz, $^3J_{HH}$ = 4.4 Hz, 1H), 4.34 (dd, $^2J_{HH}$ = 11.7 Hz, $^3J_{HH}$ = 1.87 Hz, 1H), 3.18 (m, 1H), 2.87 (t, $^3J_{HH}$ = 8.1 Hz, 2H), 1.73 (t, $^3J_{HH}$ = 8.7 Hz, 1H). δ_C (50 MHz, $CDCl_3$, ppm): 156.51, 147.13, 114.45, 113.96, 101.63, 67.21, 39.47. MS (70 eV) *m/z* (%): 204 (64) [M^+], 157 (79) [$C_6H_5OS_2^{+\bullet}$], 73 (100) [$C_3H_5S^{+\bullet}$].

Synthesis of EOTT-F_n and EOTT-H. *N*-(3-Dimethylaminopropyl)-*N*′-ethylcarbodiimide hydrochloride (EDC) (0.3 mg, 1.5 mmol) was added to a solution containing the corresponding acid (1.5 mmol) in dichloromethane. After the mixutre was stirred for 30 mn at room temperature, (2,3-dihydrothieno[3,4-*b*][1,4]oxathiin-3-yl)methanethiol (0.31 g, 1.5 mmol) was added. After a day, the solvent was removed and the crude was purified by column chromatography (silica gel; eluent: dichloromethane) to yield the products.

EOTT-F_8: *S*-((2,3-Dihydrothieno[3,4-*b*][1,4]oxathiin-3-yl)-methyl) 4,4,5,5,6,6,7,7,8,8,9,9,10,10,11,11,11-Heptadecafluoroundecanethioate. Yield 40%; r.t. 19.4 min; white solid; mp 71.2 °C. δ_H (200 MHz, $CDCl_3$, ppm): 6.75 (d, $^4J_{HH}$ = 3.5 Hz, 1H), 6.51 (d, $^4J_{HH}$ = 3.5 Hz, 1H), 4.42 (dd, $^2J_{HH}$ = 11.5 Hz, $^3J_{HH}$ = 2.0 Hz, 1H), 4.28 (m, 1H), 3.28 (m, 3H), 2.93 (t, $^3J_{HH}$ = 7.6 Hz, 2H), 2.50 (tt, $^3J_{HH}$ = 7.6 Hz, $^3J_{HF}$ = 14.8 Hz, 1H). δ_C (50 MHz, $CDCl_3$, ppm): 195.81, 147.87, 115.66, 114.67, 102.81, 68.73, 36.97, 34.58, 31.58, 26.26. δ_F ($CDCl_3$, ppm): −80.77 (m, 3F), −114.43 (m, 2F), −121.91 (m, 2F), −122.76 (m, 2F), −123.39 (m, 2F), −126.18 (m, 2F). FTIR (main vibrations): ν = 2961, 2926, 2861, 1687 (SC═O), 1535, 1447, 1422, 1223, 1197, 1145. MS (70 eV) *m/z* (%): 678 (39) [M^+], 475 (6) [$C_{11}H_4OF_{17}^{+\bullet}$], 203 (9) [$C_7H_7OS_3^{+\bullet}$], 170 (100) [$C_7H_6OS_2^+$], 157 (30) [$C_6H_5OS_2^{+\bullet}$], 73 (90) [$C_3H_5S^{+\bullet}$].

EOTT-F_6: *S*-((2,3-Dihydrothieno[3,4-*b*][1,4]oxathiin-3-yl)-methyl) 4,4,5,5,6,6,7,7,8,8,9,9,9-Tridecafluorononanethioate. Yield 42%; r.t. 18.6 min; white solid; mp 45.6 °C. δ_H (200 MHz, $CDCl_3$, ppm): 6.75 (d, $^4J_{HH}$ = 3.5 Hz, 1H), 6.51 (d, $^4J_{HH}$ = 3.5 Hz, 1H), 4.42 (dd, $^2J_{HH}$ = 11.5 Hz, $^3J_{HH}$ = 2.0 Hz, 1H), 4.29 (m, 1H), 3.28 (m, 3H), 2.93 (t, $^3J_{HH}$ = 7.6 Hz, 2H), 2.50 (tt, $^3J_{HH}$ = 7.6 Hz, $^3J_{HF}$ = 14.8 Hz, 1H). δ_C (50 MHz, $CDCl_3$, ppm): 195.80, 147.87, 115.66, 114.66, 102.81, 68.73, 36.96, 34.65, 31.58, 26.26. δ_F ($CDCl_3$, ppm): −80.70 (m, 3F), −114.44 (m, 2F), −121.92 (m, 2F), −122.90 (m, 2F), −123.50 (m, 2F), −126.17 (m, 2F). FTIR (main vibrations): ν = 2955, 2922, 2852, 1686 (SC═O), 1536, 1448, 1423, 1230, 1181, 1142. MS (70 eV) *m/z* (%): 578 (12) [M^+], 375 (2) [$C_9H_4OF_{13}^{+\bullet}$], 203 (9) [$C_7H_7OS_3^{+\bullet}$], 170 (100) [$C_7H_6OS_2^+$], 157 (35) [$C_6H_5OS_2^{+\bullet}$], 73 (100) [$C_3H_5S^{+\bullet}$].

EOTT-F_4: *S*-((2,3-Dihydrothieno[3,4-*b*][1,4]oxathiin-3-yl)-methyl) 4,4,5,5,6,6,7,7,7-Nonafluoroheptanethioate. Yield 35%; r.t. 17.4 min; white solid; mp 27.2 °C. δ_H (200 MHz, $CDCl_3$, ppm): 6.74 (d, $^4J_{HH}$ = 3.5 Hz, 1H), 6.51 (d, $^4J_{HH}$ = 3.5 Hz, 1H), 4.42 (dd, $^2J_{HH}$ = 11.5 Hz, $^3J_{HH}$ = 2.0 Hz, 1H), 4.28 (m, 1H), 3.28 (m, 3H), 2.93 (t, $^3J_{HH}$ = 7.7 Hz, 2H), 2.50 (tt, $^3J_{HH}$ = 7.7 Hz, $^3J_{HF}$ = 14.8 Hz, 1H). δ_C (50 MHz, $CDCl_3$, ppm): 195.79, 147.87, 115.66, 114.66, 102.81, 68.73, 36.96, 34.63, 31.58, 26.8. δ_F ($CDCl_3$, ppm): −81.00 (m, 3F), −114.63 (m, 2F), −124.39 (m, 2F), −126.03 (m, 2F). FTIR (main vibrations): ν = 2961, 2927, 2845, 1692 (SC═O), 1536, 1454, 1423, 1212, 1182, 1132. MS (70 eV) *m/z* (%): 478 (13) [M^+], 275 (4) [$C_7H_4OF_9^{+\bullet}$], 203 (8) [$C_7H_7OS_3^{+\bullet}$], 170 (100) [$C_7H_6OS_2^+$], 157 (40) [$C_6H_5OS_2^{+\bullet}$], 73 (83) [$C_3H_5S^{+\bullet}$].

EOTT-F_2: *S*-(2,3-Dihydrothieno[3,4-*b*][1,4]oxathiin-3-yl)-methyl 4,4,5,5,5-Pentafluoropentanethioate. Yield 25%; r.t. 16.5 min; colorless liquid. δ_H (200 MHz, $CDCl_3$, ppm): 6.76 (d, $^4J_{HH}$ = 3.5 Hz, 1H), 6.51 (d, $^4J_{HH}$ = 3.5 Hz, 1H), 4.42 (m, 1H), 4.28 (m, 1H), 3.28 (m, 3H), 2.91 (t, $^3J_{HH}$ = 7.7 Hz, 2H), 2.45 (tt, $^3J_{HH}$ = 7.7 Hz, $^3J_{HF}$ = 17.8 Hz, 1H). δ_C (50 MHz, $CDCl_3$, ppm): 195.78, 147.84, 115.65, 114.64, 102.81, 68.70, 36.93, 34.74, 31.54, 26.02. δ_F ($CDCl_3$, ppm): −85.43 (s, 3F), −118.44 (t, 2F). FTIR (main vibrations): ν = 2959, 2932, 2854, 1691 (SC═O), 1534, 1454, 1427, 1286, 1187, 1095. MS (70 eV) *m/z* (%): 378 (5) [M^+], 203 (8) [$C_7H_7OS_3^{+\bullet}$], 175 (27) [$C_5H_4OF_5^{+\bullet}$], 170 (90) [$C_7H_6OS_2^+$], 157 (44) [$C_6H_5OS_2^{+\bullet}$], 73 (100) [$C_3H_5S^{+\bullet}$].

EOTT-H: *S*-(2,3-Dihydrothieno[3,4-*b*][1,4]oxathiin-3-yl)-methyl Propanethioate. Yield 23%; r.t. 16.5 min; colorless liquid.

Scheme 1. (a) Previously Reported EDOT and (b) Synthesized EOTT Derivatives

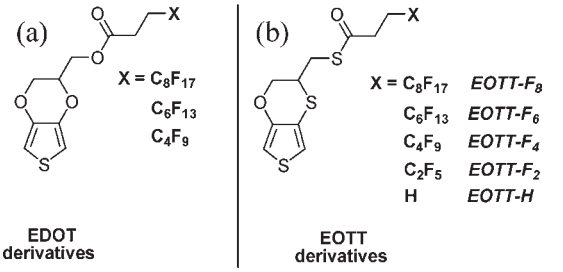

Scheme 2. Synthetic Route to the Monomers (n = 2, 4, 6, 8)

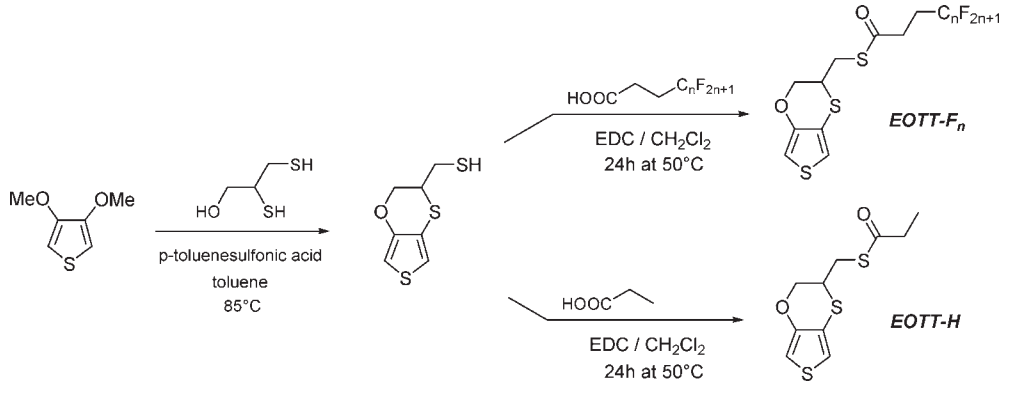

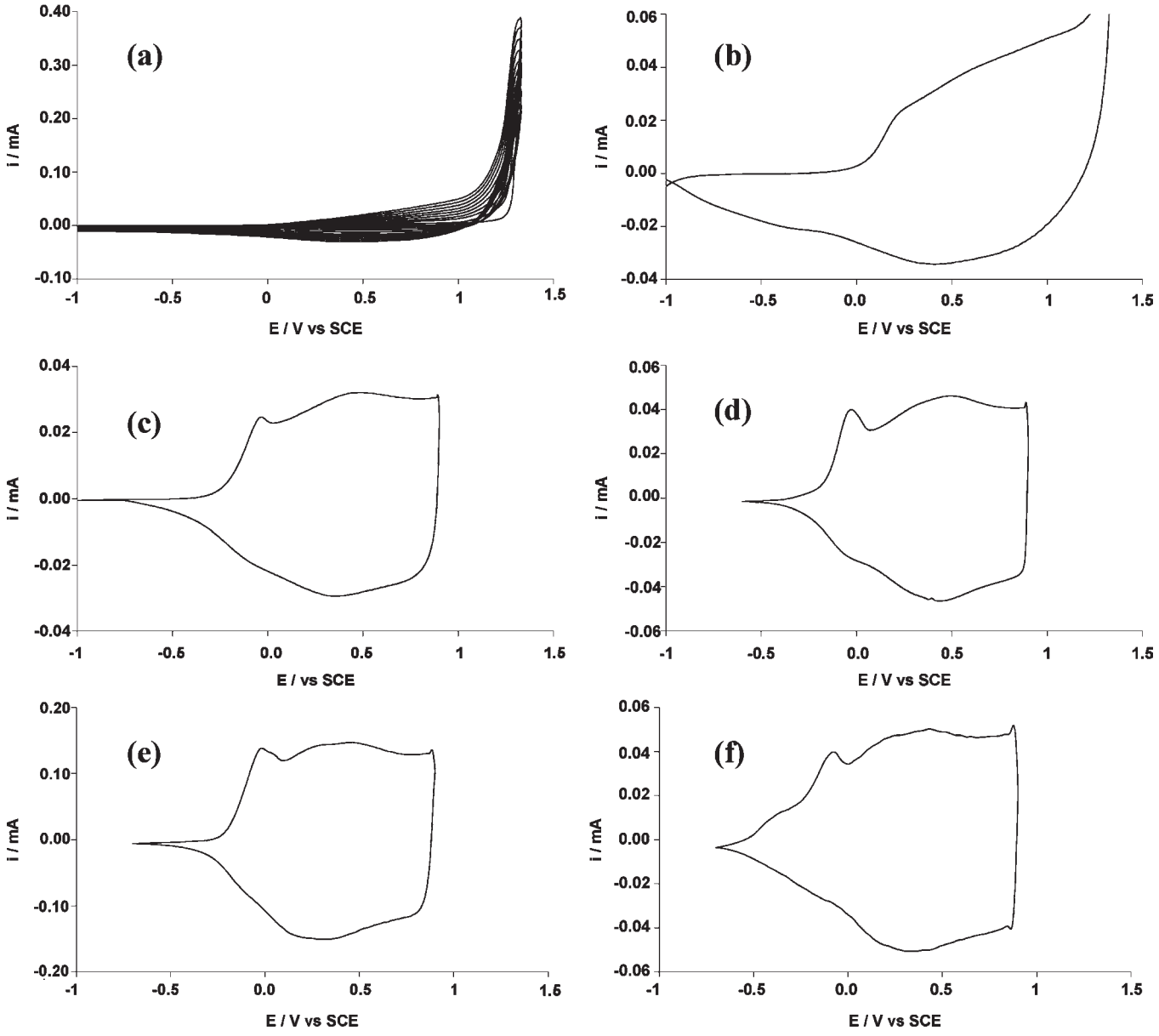

Figure 1. (a) Cyclic voltammogram of EOTT-F_8 (0.01 M) on a Pt electrode recorded in 0.1 M Bu4NPF_6/CH_3CN and cyclic voltammograms of (b) PEOTT-F_8, (c) PEOTT-F_6, (d) PEOTT-F_4, (e) PEOTT-F_2, and (f) PEOTT-H in 0.1 M Bu_4NPF_6/CH_3CN solution without monomer.

δ_H (200 MHz, $CDCl_3$, ppm): 6.73 (d, $^4J_{HH}$ = 3.5 Hz, 1H), 6.50 (d, $^4J_{HH}$ = 3.5 Hz, 1H), 4.40 (dd, $^2J_{HH}$ = 11.7 Hz, $^3J_{HH}$ = 3.9 Hz, 1H), 4.27 (m, 1H), 3.27 (m, 3H), 2.62 (q, $^3J_{HH}$ = 7.5 Hz, 2H), 1.19 (t, $^3J_{HH}$ = 7.5 Hz, 3H). δ_C(50 MHz, $CDCl_3$, ppm): 199.50, 147.97, 115.46, 115.03, 102.62, 68.88, 37.47, 37.17, 31.13, 9.55. FTIR (main vibrations): ν = 2974, 2928, 2881, 1695 (SC═O), 1536, 1454, 1421, 1181, 1155. MS (70 eV) m/z (%): 260 (5) [M^+], 170 (36) [$C_7H_6OS_2^+$], 157 (11) [$C_6H_5OS_2^{+\bullet}$], 73 (32) [$C_3H_5S^{+\bullet}$], 57 (100) [$C_3H_5O^{+\bullet}$].

Electrodeposition Experiments. Ten milliliters of a solution of tetrabutylammonium hexafluorophosphate (0.1 M) in anhydrous acetonitrile was put in a glass cell and degassed with argon for 30 min. Next, 10 mM of monomer was added, and the solution was degassed for another 10 min. A three-electrode system (a platinum disk working electrode, a glassy carbon counter-electrode, and a SCE reference electrode) was inserted in the cell and connected to an Autolab PGSTAT 30 potentiostat from Eco Chemie B.V.

RESULTS AND DISCUSSION

Synthesis. The monomers were synthesized in two steps from 3,4-dimethoxythiophene. The first step is the transetherification of 3,4-dimethoxythiophene with 2,3-dimercapto-1-propanol in refluxing toluene (three days) and with *p*-toluenesulfonic acid. 2,3-Dimercapto-1-propanol (3 equiv) was added three times to avoid the formation of dimers. (2,3-Dihydrothieno[3,4-*b*]-[1,4]oxathiin-3-yl)methanethiol (Scheme 2) was isolated by column chromatography, and the presence of this compound was confirmed by ^{1}H NMR (presence of a triplet for the proton of the thiol) and mass spectrometry (loss of CH_2−SH fragments; cf., Supporting Information). This original platform molecule can be used for many applications. Other isomers could, maybe, be obtained with this process by controlling the reaction parameters, and this study will be realized in the future. The monomers EOTT-F_n and EOTT-H were then

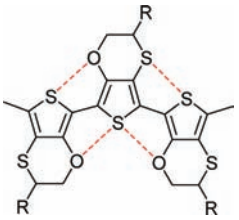

Figure 2. Schematic representation of S−O and S−S intramolecular interactions in the polymer backbone.

obtained by esterification reaction with the corresponding acids and in the presence of EDC. The obtaining of the monomers was confirmed by ^{1}H, ^{19}F, and ^{13}C NMR, infrared, and mass spectrometry.

Electrodeposition. The experiments of electrodeposition were performed in a solution of anhydrous acetonitrile containing 0.1 M of tetrabutylammonium hexafluorophosphate and 10 mM of monomer. The monomer oxidation potentials, determined by cyclic voltammetry, were 1.48 V vs SCE for EOTT-F_4, 1.45 V for EOTT-F_2, 1.42 V for EOTT-F_6, and 1.41 V for EOTT-F_8 and EOTT-H. By comparison with EDOT-F_n derivatives, the replacement of one oxygen atom by a sulfur one in the heterocycle decreased the monomer oxidation potential by about 0.15 V, due to the higher electron-donating effect of sulfur. Scanning from −1 V until a potential close to the monomer oxidation potential gave rise to a well-defined and reversible doping process, as represented in Figure 1a for EOTT-F_8, due to the electrodeposition of an electroactive polymer film on the working electrode. After rinsing, the electrodes were put in a solution without monomer to characterize the polymers. The curves obtained by cyclic voltammetry are represented in Figure 1b−f for each corresponding polymer. These curves are quite close to those obtained with EDOT-F_n derivatives, which indicates that the replacement of one oxygen atom by a sulfur one in the EDOT chemical structure does not have a significant effect on the polymerization and the doping process.[33b] These data confirm the presence of noncovalent S−O and S−S intramolecular interactions in the polymer backbone (Figure 2 gives a schematic representation of these interactions), as previously reported in the literature by analyzing the dimers between 3,4-ethylenedioxythiophene (EDOT) and 3,4-ethylenedisulfanylthiophene (EDST).[38,39] Indeed, it has been demonstrated that high intramolecular interactions were present in the dimers EDOT−EDOT (S−O interactions) and EDOT−EDST (S−O and S−S interactions) but not in the system EDST−EDST (only S−S interactions). These intramolecular interactions between oxygen and sulfur atoms are very important for the planarity of the polymers by rigidification and as a consequence their electronic and electrooptic properties.

Surface Characterization. For the determination of surface properties, the polymers were electrodeposited on larger gold surfaces by implying a constant potential and using various deposition charges (Q_s from 0 to 400 mC/cm^2). In our case, a deposition charge of 200 mC/cm^2 corresponds to a time deposition of about 2 mn (the time deposition depends on the surface area) and a polymer mass of about 1.2 mg/cm^2. To determine the film thickness, a notch was made into the surfaces, and their depth was measured by optical microscopy. For the three polymers, a depth of about 3−4 μm was determined for Q_s = 200 mC/cm^2. The coating was fragile against scratch, and the polymer adherence was relatively good but has to be improved for an industrial application.

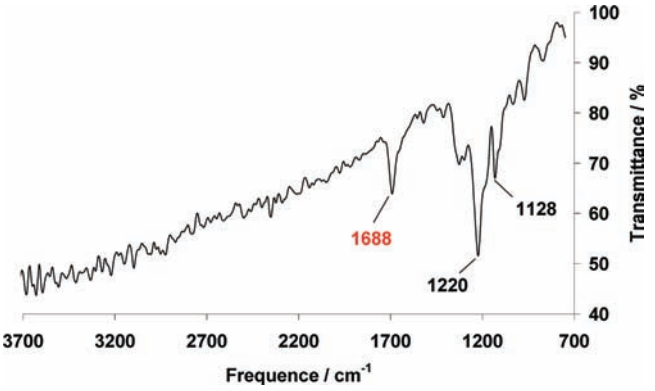

Figure 3. Infrared spectra of PEOTT-F_4 obtained by imaging infrared.

Table 1. Water-Repellent Properties for the Electrodeposited Polymers for Q_s = 100 mC/cm^2[a]

		dynamic contact angles [deg] of water			
	static contact angles [deg] of water	advancing	receding	hysteresis	sliding angle
PEOTT-F_8	**160.4**	161.1	160.3	**0.8**	**1.9**
PEOTT-F_6	**160.7**	161.0	158.7	**2.3**	**2.1**
PEOTT-F_4	**158.9**	159.0	133.6	25.4	17.6
PEOTT-F_2	117.3				
PEOTT-H	66.7				

[a] Static and dynamic contact angles were measured with 2 and 6 μL water droplets, respectively.

The polymer was characterized by infrared. Because the presence of the charges and the counterions induces the presence of large bands in the infrared spectra, the polymers were, first, dedoped by imposed potential (−1 V for 1 h). An example of infrared spectra is given in Figure 3. The presence of the polymer was confirmed especially with the presence of the thioester band at 1688 cm^{-1} and the fluorinated chains at 1128 cm^{-1}.

Surface Wetting. For Q_s = 100 mC/cm^2, the polymeric surfaces PEOTT-F_8, PEOTT-F_6, and PEOTT-F_4 displayed superhydrophobic properties with static contact angles of water (CA_{water}) above 158°, while PEOTT-F_2 was hydrophobic (CA_{water} = 117.3°) and PEOTT-H hydrophilic (CA_{water} = 66.7°), as shown in Table 1. Hence, the increase in CA_{water} was very important between a *F*-ethyl and a *F*-butyl chain. However, the influence of the *F*-alkyl chain is relatively limited between a *F*-butyl, a *F*-hexyl, or a *F*-octyl chain. The dynamic contact angle measurements revealed the extremely low hysteresis (H < 3°) and sliding angles (α < 3°) of PEOTT-F_8 and PEOTT-F_6. The hysteresis and sliding angle were higher for PEOTT-F_4 (H = 25.4°, α = 17.6°). In comparison with the previously reported PEDOT-F_n derivatives,[33b] the water antiwetting properties were quite similar with a *F*-hexyl and a *F*-octyl chain but slightly lower with a *F*-butyl chain.

Next, the polymers were deposited with various Q_s values as shown in Figure 4. In this graph, it can be deduced that a Q_s of 50 mC/cm^2 was necessary to reach the best CA_{water} for PEOTT-F_8

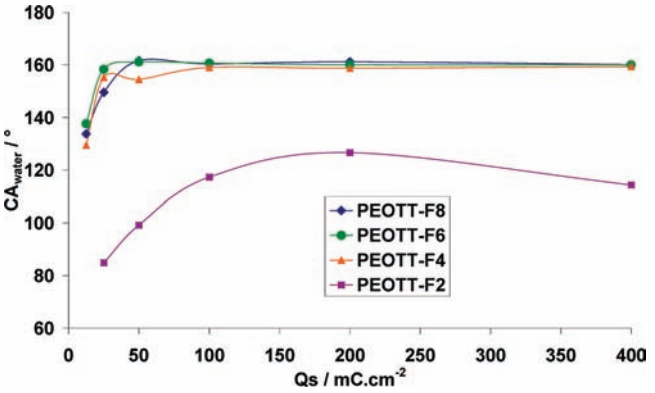

Figure 4. Influence of the deposition charge (Q_s) on the static contact angle of water (CA_{water}) for the fluorinated polymers.

and PEOTT-F_6, 100 mC/cm^2 for PEOTT-F_4, and 200 mC cm^{-2} for PEOTT-F_2. It is also very important to note the possibility of reaching CA_{water} above 125° with extremely short *F*-ethyl chains.

This work confirms the possibility of using short fluorinated chains (*F*-butyl and *F*-ethyl) to reach extremely interesting antiwetting properties. The main interest of using short fluorinated chains is to reduce the eco-toxicity of superhydrophobic materials. Indeed, among all of the literature on superhydrophobic surfaces, the surface hydrophobization was mainly performed with fluorinated agents containing long fluorinated tails. However, the high persistence and bioaccumulative potential of fluorinated compounds has been demonstrated in a variety of wildlife, especially the fluorinated chains of length above seven fluoromethylene units.[40,41]

To understand the wettability of these surfaces, the contact angle measurements were correlated to surface morphologies.

Surface Morphology and Roughness. The surface morphology was investigated by SEM. The SEM images of polymer films are gathered in Figures 5 and 6. A very significant change in morphology was observed as a function of the fluorinated chain length. The surface morphology was extremely microstructured for PEOTT-F_2 but not nanostructured (the film contained pores larger than 2 μm), consisting of assemblies of very long fibers for PEOTT-F_4 (length: not determinable, $\varnothing \approx 300$ nm), small fibers for PEOTT-F_6 of quite the same diameter (length ≈ 1 μm, $\varnothing \approx$ 300 nm), and a mixture of smaller fibers (length ≈ 0.5 μm, $\varnothing \approx$ 150 nm) and cauliflower-like structure for PEOTT-F_8. By contrast, PEOTT-H can be considered as not structured, as shown in Figure 6, which means that the presence of the fluorinated chains is very important for the surface construction. A change in morphology with the fluorinated chain length was already observed in the EDOT-F_n series (cf., Supporting Information).[33b] By comparing the films observed with these two series, a spectacular modification of the surface morphology was observed with the monomers substituted with a *F*-butyl tail: thin fibrils for EDOT-F_4 and very long fibers for EOTT-F_4 (Figure 7 shows the surface morphology comparison). Moreover, as shown in Figure 6, the long fibers obtained with EOTT-F_4 were not smooth but resembled assemblies of long plated fibers. The diameter was quite the same for all of the fibers (~300 nm). These characteristics are close to fibrous structures observed in natural superhydrophobic surfaces[42−44] and more precisely at the surface of *Drosera burmanni* leaves.[42] It is also important to note that among all of the monomers previously tested using the same electrochemical conditions,[30−34] this is the first time that this

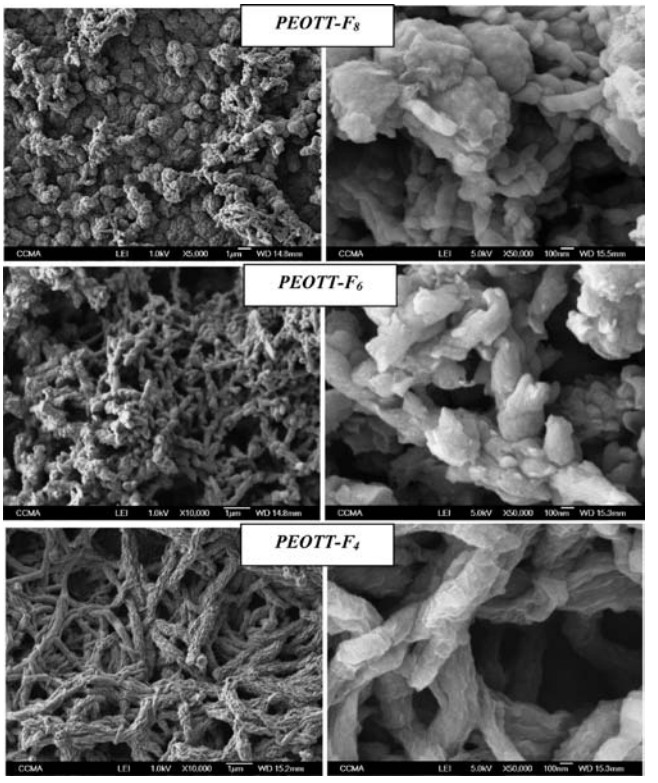

Figure 5. SEM images of PEOTT-F_8, PEOTT-F_6, and PEOTT-F_4; magnification ×10 000 and ×50 000; Q_s = 200 mc/cm^2; salt: Bu_4NPF_6.

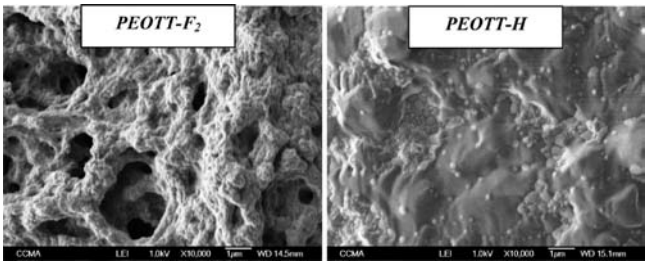

Figure 6. SEM images of PEOTT-F_2 and PEOTT-H; magnification × 10 000; Q_s = 200 mc/cm^2; salt: Bu_4NPF_6.

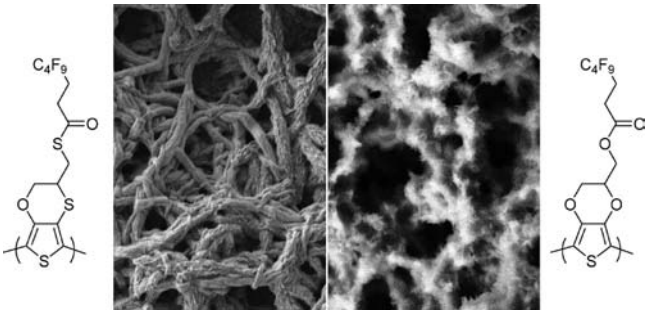

Figure 7. Surface morphology comparison between PEOTT-F_4 and PEDOT-F_4, electrodeposited with the same conditions.

surface morphology has been obtained (some examples of surface morphologies as a function of the monomer are given in the Supporting Information). If electrospinning[19,45−47] is known as a

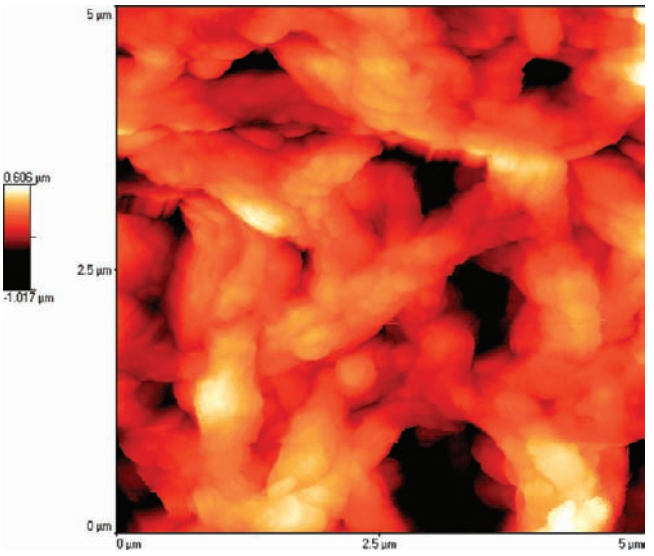

Figure 8. AFM image of PEOTT-F_4; area 5 μm × 5 μm.

conventional method to deposit fibers on surfaces by applying a high voltage, this is not the case for the electrodeposition (see the Supporting Information, Figures ESI7,8). Indeed, if the presence of hydrogen bonding is known to be indispensable for the formation of polyaniline fibers,[48] here the fibers were obtained, in part, thanks to the presence of sulfur atoms. It seems that the presence of sulfur atoms in the monomer structure allowed one to aggregate thin fibrils into extremely long fibers. The presence of supplementary sulfur atoms in the monomer structure may increase the S−O and S−S intra- and intermolecular interactions, for example, with the oxygen atom of the thioester function, as observed in ester substituted bithiophenes.[49] As a consequence, these supplementary interactions may switch the surface morphology from thin fibrils to extremely long plated fibers. Moreover, the length of the polymer fibers can be controlled with the length of the fluorinated chain.

To better understand the effect of the surface roughness on the surface wettability, the surfaces were analyzed by optical profilometry and atomic force microscopy (AFM). The micrometric surface roughness (R_a and R_q) was determined by optical profilometry. The analyzed surface areas were 182 μm × 239 μm. The arithmetic surface roughness (R_a) is of the same magnitude as the fluorinated chain length: R_a = 2.4 μm and R_q = 3.3 μm for PEOTT-F_8, R_a = 2.1 μm and R_q = 2.5 μm for PEOTT-F_6, and R_a = 1.9 μm and R_q = 3.5 μm for PEOTT-F_4.

The submicronic surface roughness (R_a and R_q) was determined by AFM. This time, the surface areas were 5 μm × 5 μm. A decrease of the surface roughness was also measured as a function of the alkyl chain length decrease: R_a = 0.39 μm and R_q = 0.49 μm for PEOTT-F_8, R_a = 0.27 μm and R_q = 0.36 μm for PEOTT-F_6, and R_a = 0.18 μm and R_q = 0.23 μm for PEOTT-F_4. These analyses also confirm the presence of long plated fibers in the case of PEOTT-F_4 as shown in Figure 8. These surface analyses show the importance of the surface roughness on the static and especially dynamic contact angles of water. In this study, a high surface roughness seems to be necessary to reach self-cleaning surfaces (hysteresis and sliding angle below 10°).

To better understand the influence of the surface roughness/morphology and the chemical part on the surface wettability, it is necessary to produce smooth films of the polymers. Because the

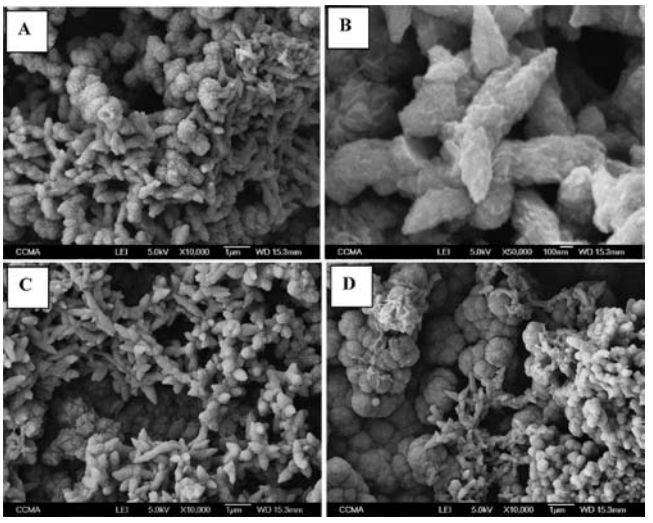

Figure 9. SEM images of PEOTT-F_4 obtained with $Bu_4NCF_3SO_3$ ((A) ×10 000 and (B) ×50 000), $Bu_4NC_4F_9SO_3$ ((C) ×10 000), and $Bu_4NC_8F_{17}SO_3$ ((D) × 10 000); Q_s = 200 mc/cm^2.

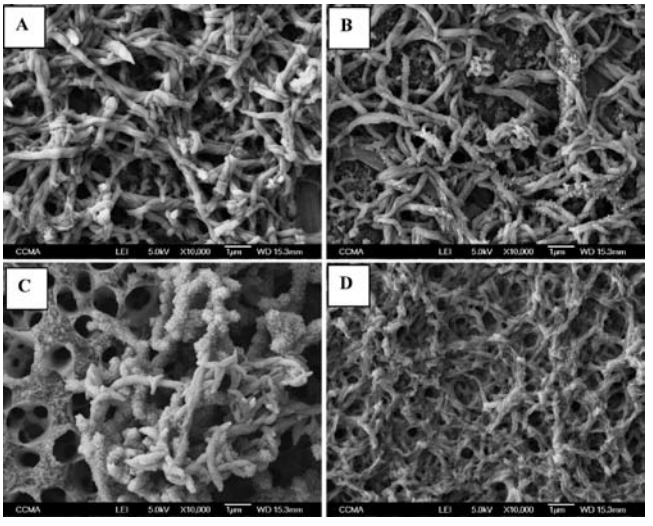

Figure 10. SEM images of PEOTT-F_4 obtained with (A) benzonitrile, (B) nitrobenzene, (C) dichloromethane, and (D) propylene carbonate as solvent; magnification ×10 000; Q_s = 200 mc/cm^2.

polymers were not soluble, we have chosen EOTT-F_4 as a reference monomer and tried to form smooth films by changing electrochemical parameters and more precisely the salt and the solvent. These changes also allowed one to tune the surface morphology and wettability.

Influence of Electrochemical Conditions. By changing Bu_4NPF_6 as salt for Bu_4NBF_4, Bu_4NClO_4, $Bu_4NCF_3SO_3$, $Bu_4NC_4F_9SO_3$, and $Bu_4NC_8F_{17}SO_3$, superhydrophobic surfaces with contact angles of water between 159° and 161° were obtained. Hence, the influence of the salt on the water-repellency properties is minor, but the salt has an important influence on the surface morphology. Whereas long fibers were only observed using Bu_4NPF_6, shorter fibers or needles were obtained with all of the other salts; Figure 9B shows the presence of nanostructured needles (length ≈ 700 nm) for films obtained with $Bu_4NCF_3SO_3$ (SEM images with other salts are given in the

Supporting Information). The films also contained cauliflower-like or flower-like microstructures.

By changing acetonitrile as solvent for benzonitrile, nitrobenzene, dichloromethane, and propylene carbonate, we observed a more important influence of the solvent on the water-repellency properties. Superhydrophobic surfaces were elaborated with all of the solvents except with propylene carbonate (CA_{water} = 156° with nitrobenzene and dichloromethane, 153° with benzonitrile, and 138° with propylene carbonate). Long polymer fibers were obtained not only with acetonitrile but also with benzonitrile (Figure 10A) and nitrobenzene (Figure 10B) with quite the same diameter as that obtained with acetonitrile. However, these electrochemical changes did not produce smooth surfaces, which means that the ability of these monomers to form structured surfaces by electrodeposition is exceptional. Moreover, the structure of these monomers is oriented to form fibrous structures using a very large range of electrochemical conditions.

CONCLUSIONS

The control of the surface properties, both morphology and wettability, is extremely important in the design of superhydrophobic surfaces for many practical applications. Here, we have reported the synthesis and characterization of original 3,4-ethyleneoxythiathiophenes (EOTT) as platform molecules and its derivatives containing semifluorinated chain of various length (*F*-octyl, *F*-hexyl, *F*-butyl, and *F*-ethyl). These monomers were electropolymerized to form in one step superhydrophobic or highly hydrophobic films.

We have shown that it is possible to fabricate surprisingly extremely long polymer fibers by electrodeposition of fluorinated EOTT derivatives; control the length of the polymer fibers and the superhydrophobic properties of the films with the length of the fluorinated chains and electrochemical conditions; switch the surface morphology from thin fibrils to extremely long fibers by incorporating sulfur atoms in the monomer structure; and demonstrate the use of fluorinated materials of low chain length to reach superhydrophobic properties and create surfaces with *F*-ethyl chains displaying exceptional antiwetting properties (contact angle above 125°).

If the general procedure is the use of highly fluorinated tails to reach hydrophobic to superhydrophobic properties, here we demonstrate the ability of low fluorine containing monomers to build-up superhydrophobic material and their ability to form fiber mats from a one-pot method. This work opens new ways for the preparation of self-made surfaces for antiwetting properties.

ASSOCIATED CONTENT

Supporting Information. General information, mass spectra of molecules, and complementary SEM images. This material is available free of charge via the Internet at http://pubs.acs.org.

AUTHOR INFORMATION

Corresponding Author
frederic.guittard@unice.fr

ACKNOWLEDGMENT

We thank Jean-Pierre Laugier of the Centre Commun de Microscopie Appliquée (CCMA, University of Nice — Sophia Antipolis) for the SEM images. T.D. also thanks Elena Celia for the AFM analyses.

REFERENCES

(1) (a) Bhushan, B. *Philos. Trans. R. Soc., A* **2009**, *367*, 1445–1486. (b) Bhushan, B.; Jung, Y. C.; Koch, K. *Philos. Trans. R. Soc., A* **2009**, *367*, 1631–1672.

(2) (a) Sun, B.; Mi, Z.-T.; An, G.; Liu, G.; Zou, J.-J. *Ind. Eng. Chem. Res.* **2009**, *48*, 9823–9829. (b) Causa, F.; Battista, E.; Della Moglie, R.; Guarnieri, D.; Iannone, M.; Netti, P. A. *Langmuir* **2010**, *12*, 9875–9884.

(3) (a) Zhang, Z.; Chen, S.; Jiang, S. *Biomacromolecules* **2006**, *7*, 3311–3315. (b) Miessner, M.; Peter, M. G.; Vincent, J. F. V. *Biomacromolecules* **2001**, *2*, 369–372.

(4) (a) Louloudi, M.; Deligiannakis, Y.; Hadjiliadis, N. *Inorg. Chem.* **1998**, *37*, 6847–6851. (b) Ma, P. X. *Adv. Drug Delivery Rev.* **2008**, *60*, 184–198.

(5) (a) Liu, K.; Jiang, L. *Nanoscale* **2011**, *3*, 825–838. (b) Liu, K.; Yao, X.; Jiang, L. *Chem. Soc. Rev.* **2010**, *39*, 3240–3255. (c) Liu, M.; Jiang, L. *Adv. Funct. Mater.* **2010**, *20*, 3753–3764.

(6) (a) Liu, M.; Zheng, Y.; Zhai, J.; Jiang, L. *Acc. Chem. Res.* **2010**, *43*, 368–377. (b) Guo, Z.; Liu, W.; Su, B.-L. *J. Colloid Interface Sci.* **2011**, *353*, 335–355.

(7) Crick, C. R.; Parkin, I. P. *Chem.-Eur. J.* **2010**, *16*, 3568–3588.

(8) Gao, X.; Yan, X.; Yao, X.; Xu, L.; Zhang, K.; Zhang, J.; Yang, B.; Jiang, L. *Adv. Mater.* **2007**, *19*, 2213–2217.

(9) Kako, T.; Nakajima, A.; Irie, H.; Kato, Z.; Uematsu, K.; Watanabe, T.; Hashimoto, K. *J. Mater. Sci.* **2004**, *39*, 547–555.

(10) (a) Hoefnagels, H. F.; Wu, D.; de With, G.; Ming, W. *Langmuir* **2007**, *23*, 13158–13163. (b) Leng, B.; Shao, Z.; de With, G.; Ming, W. *Langmuir* **2009**, *25*, 2456–2460.

(11) (a) Satam, D.; Lee, H. J.; Wilusz, E. *AATCC Rev.* **2010**, *10*, 59–63. (b) Lee, H. J.; Willis, C. *Chem. Ind.* **2009**, *7*, 21–23.

(12) (a) Chen, Y.; Chen, S.; Yu, F.; Sun, W.; Zhu, H.; Yin, Y. *Surf. Interface Anal.* **2009**, *41*, 872–877. (b) Ishizaki, T.; Hieda, J.; Saito, N.; Saito, N.; Takai, O. *Electrochim. Acta* **2010**, *55*, 7094–7101.

(13) Genzer, J.; Efimenko, K. *Biofouling* **2006**, *22*, 339–360.

(14) Öner, D.; McCarthy, T. J. *Langmuir* **2000**, *16*, 7777–7782.

(15) Martines, E.; Seunarine, K.; Morgan, H.; Gadegaard, N.; Wilkinson, C. D. W.; Riehle, M. O. *Nano Lett.* **2005**, *5*, 2097–2103.

(16) Liu, B.; He, Y.; Fan, Y.; Wang, X. *Macromol. Rapid Commun.* **2006**, *27*, 1859–1864.

(17) Amigoni, S.; Taffin de Givenchy, E.; Dufay, M.; Guittard, F. *Langmuir* **2009**, *25*, 11073–11077.

(18) Sun, M.; Luo, C.; Xu, L.; Ji, H.; Ouyang, Q.; Yu, D.; Chen, Y. *Langmuir* **2005**, *21*, 8978–8981.

(19) Jiang, L.; Zhao, Y.; Zhai, J. *Angew. Chem., Int. Ed.* **2004**, *43*, 4338–4341.

(20) Sun, M.; Luo, C.; Xu, L.; Ji, H.; Ouyang, Q.; Yu, D.; Chen, Y. *Langmuir* **2005**, *21*, 8978–8981.

(21) Taffin de Givenchy, E.; Amigoni, S.; Martin, C.; Andrada, G.; Caillier, L.; Geribaldi, S.; Guittard, F. *Langmuir* **2009**, *25*, 6448–6453.

(22) Zhu, Y.; Hu, D.; Wan, M.; Jiang, L.; Wei, Y. *Adv. Mater.* **2007**, *19*, 2092–2096.

(23) Zhu, Y.; Li, J.; Wan, M.; Jiang, L. *Macromol. Rapid Commun.* **2008**, *29*, 239–243.

(24) Wan, M. *Adv. Mater.* **2008**, *20*, 2926–2932.

(25) Qu, M.; Zhao, G.; Cao, X.; Zhang, J. *Langmuir* **2008**, *24*, 4185–4189.

(26) Zhong, W.; Wang, Y.; Yan, Y.; Sun, Y.; Deng, J.; Yang, W. *J. Phys. Chem. B* **2007**, *111*, 3918–3926.

(27) Bok, H.-M.; Shin, T.-Y.; Park, S. *Chem. Mater.* **2008**, *20*, 2247–2251.

(28) (a) Yu, W.; Yao, T.; Xiao, L.; Wang, T.; Gao, H.; Zhang, J.; Yang, B. *J. Appl. Polym. Sci.* **2011**, *119*, 1052–1059. (b) Yan, H.; Kurogi, K.; Tsujii, K. *Colloids Surf., A* **2007**, *292*, 27–31.

(29) (a) Xu, L.; Chen, W.; Mulchandani, A.; Yan, Y. *Angew. Chem., Int. Ed.* **2005**, *44*, 6009–6012. (b) Xu, L.; Chen, Z.; Chen, W.; Mulchandani, A.; Yan, Y. *Macromol. Rapid Commun.* **2008**, *29*, 832–838.

(30) (a) Darmanin, T.; Guittard, F. *J. Am. Chem. Soc.* **2009**, *131*, 7928–7933. (b) Darmanin, T.; Guittard, F. *J. Mater. Chem.* **2009**, *19*, 7130–7136.
(31) Zenerino, A.; Darmanin, T.; Taffin de Givenchy, E.; Amigoni, S.; Guittard, F. *Langmuir* **2010**, *26*, 13545–13549.
(32) (a) Darmanin, T.; Taffin de Givenchy, E.; Guittard, F. *Macromolecules* **2010**, *43*, 9365–9370. (b) Darmanin, T.; Guittard, F. *Langmuir* **2009**, *25*, 5463–5466.
(33) (a) Darmanin, T.; Taffin de Givenchy, E.; Amigoni, S.; Guittard, F. *Langmuir* **2010**, *26*, 17596–17602. (b) Darmanin, T.; Nicolas, M.; Guittard, F. *Langmuir* **2008**, *24*, 9739–9746.
(34) (a) Yan, H.; Kurogi, K.; Mayama, H.; Tsujii, K. *Angew. Chem., Int. Ed.* **2005**, *44*, 3453–3456. (b) Kurogi, K.; Yan, H.; Mayama, H.; Tsujii, K. *J. Colloid Interface Sci.* **2007**, *312*, 156–163.
(35) Chiba, K.; Kurogi, K.; Monde, K.; Hashimoto, M.; Yoshida, M.; Mayama, H.; Tsujii, K. *Colloids Surf., A* **2010**, *354*, 234–239.
(36) Luo, S.-C.; Liour, S. S.; Yu, H.-H. *Chem. Commun.* **2010**, *46*, 4731–4733.
(37) Blanchard, P.; Cappon, A.; Levillain, E.; Nicolas, Y.; Frere, P.; Roncali, J. *Org. Lett.* **2002**, *4*, 607–609.
(38) Skotheim, T. A.; Reynolds, J. R. *Handbook of Conducting Polymers, Conjugated Polymers: Theory, Synthesis, Properties and Characterization*, 3rd ed.; CRC Press Taylor & Francis Group: Boca Raton, FL, 2007.
(39) (a) Turbiez, M.; Frère, P.; Allain, M.; Gallego-Planas, N.; Roncali, J. *Macromolecules* **2005**, *38*, 6806–6912. (b) Raimundo, J.-M.; Blanchard, P.; Frère, P.; Mercier, N.; Ledoux-Rak, I.; Hierle, R.; Roncali, J. *Tetrahedron Lett.* **2001**, *42*, 1507–1510.
(40) (a) Houde, M.; Martin, J. W.; Letcher, R. J.; Solomon, K. R.; Muir, D. C. G. *Environ. Sci. Technol.* **2006**, *40*, 3463–3473. (b) Giesy, J. P.; Kannan, K. *Environ. Sci. Technol.* **2001**, *35*, 1339–1342.
(41) (a) Conder, J. M.; Hoke, R. A.; de Wolf, W.; Russell, M. H.; Buck, R. C. *Environ. Sci. Technol.* **2008**, *42*, 995–1003. (b) Kudo, N.; Kawashima, Y. *J. Toxicol. Sci.* **2003**, *28*, 49–57.
(42) Barthlott, W.; Neinhuis, C.; Cutler, D.; Ditsch, F.; Meusel, I.; Theisen, I.; Wilhelmi, H. *Bot. J. Lin. Soc.* **1998**, *126*, 237–260.
(43) Gu, Z.; Wei, H.; Zhang, R.; Han, G.; Pan, C.; Zhang, H.; Tian, X.; Chen, Z. *Appl. Phys. Lett.* **2005**, *86*, 201915.
(44) Miyauchi, Y.; Ding, B.; Shiratori, S. *Nanotechnology* **2006**, *17*, 5151–5156.
(45) Ma, M.; Mao, Y.; Gupta, M.; Gleason, K. K.; Rutledge, G. C. *Macromolecules* **2005**, *38*, 9742–9748.
(46) Lim, J.-M.; Yi, G.-R.; Moon, J. H.; Heo, C.-J.; Yang, S.-M. *Langmuir* **2007**, *23*, 7981–7989.
(47) Singh, A.; Steely, L.; Allcock, H. R. *Langmuir* **2005**, *21*, 11604–11607.
(48) (a) Huang, J. X.; Kaner, R. B. *Nat. Mater.* **2004**, *3*, 783–786. (b) Huang, J. X.; Kaner, R. B. *Angew. Chem., Int. Ed.* **2004**, *43*, 5817–5821.
(49) Pomerantz, M.; Cheng, Y. *Tetrahedron* **1999**, *40*, 3317–3320.